“This document is the Accepted Manuscript version of a Published Work that appeared in final form in The Journal of Physical Chemistry A, copyright © American Chemical Society after peer review and technical editing by the publisher. To access the final edited and published work see https://pubs.acs.org/doi/10.1021/acs.jpca.1c03464”.

Analysis of the Complex Quadrupole Hyperfine Patterns for Two Chlorine Nuclei in the Rotational Spectrum of 2,5-Dichlorothiophene

Gabrielle Daudet and Jennifer van Wijngaarden*

Department of Chemistry, University of Manitoba, Winnipeg, Manitoba, R3T 2N2, Canada

*Corresponding author

Email: vanwijng@cc.umanitoba.ca

Phone: (204)474-8379

Fax: (204)474-7608

TOC graphic

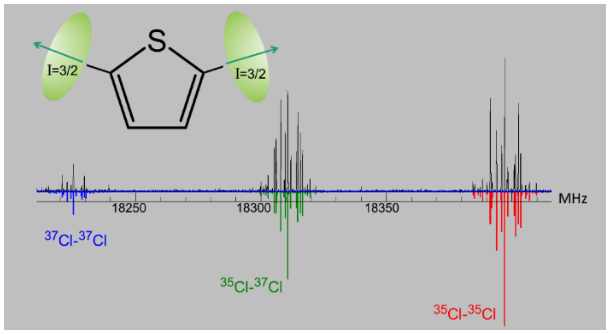

Abstract

The rotational spectrum of 2,5-dichlorothiophene (DCT) was measured for the first time using Fourier transform microwave spectroscopy from 5.5-19 GHz. Dense hyperfine splitting patterns due to the two quadrupolar chlorine nuclei (I=3/2) were resolved and assigned for the ^{35}Cl-^{35}Cl, ^{37}Cl-^{35}Cl and ^{37}Cl-^{37}Cl isotopologues as well as for the two ^{13}C and one ^{34}S analogs with two ^{35}Cl atoms allowing derivation of their respective nuclear quadrupole coupling tensors. The rotational constants obtained from fitting the spectra of the six isotopic species allowed derivation of the experimental geometry of DCT for comparison with the equilibrium structure computed at the MP2/aug-cc-pVTZ level. This revealed that the electron withdrawing effect of chlorine causes small distortions to the ring geometry relative to thiophene including a 1.1° increase in the two S-C-C angles and a 0.012 Å increase to the two S-C bonds.

Introduction

Thiophenes are important heterocyclic building blocks in the synthesis of value-added chemicals in the agriculture and pharmaceutical industries as this five-membered ring can replace the benzene moiety in certain bioactive compounds without compromising its function.[1] This is seen, for example, in drugs such as the analgesic sufentanil, the thiophene analogue of fentanyl. Halogen-substituted derivatives such as α-chlorothiophene are used by medicinal chemists to tweak the bioactivity of the heterocycle by, for example, adding a new activation site or by altering steric hindrance. Consequently, these structural motifs are found in pharmaceuticals such as the nonsteroidal anti-inflammatory drug lornoxicam, the anti-fungal medicine tioconazole and the anticoagulant rivaroxaban.[2]

In terms of their fundamental physical and chemical properties, chlorine-containing molecules hold a place of special interest for the NMR community owing to unique spectral features arising from the relatively large nuclear quadrupole moments (Q) of ^{35}Cl (-81.65(80) mbarn) and ^{37}Cl (-64.35(64) mbarn) which are both I=3/2 nuclei.[3] To avoid broad NMR line shapes, samples with a high Q nucleus in a region of high symmetry are needed to employ standard spectroscopic methods unless a single crystal can be formed. Even so, the resulting spectra often need to be interpreted in the high field limit (where the Larmor frequency is much greater than the quadrupolar frequency) requiring large magnets for data acquisition. As a result of these challenges, Bryce and Sward have highlighted an overall ‘dearth’ of experimental and quantum chemical information regarding the chemical shift tensors of chlorinated molecules.[3] The complementary technique of rotational spectroscopy offers promise of support in this regard as molecules containing high Q nuclei can be studied in isolation. Analysis of the splitting patterns arising from quadrupolar nuclei allow the derivation of accurate spectroscopic constants (eQq or χ, known as C_Q in the NMR community)[4] which describe the interaction of the nuclear quadrupole moment and the surrounding electric field gradient. The quadrupole coupling tensors of many species with a single chlorine atom including those of 2-[5] and 3-chlorothiophene,[6] for example, have been obtained in this way.

From a rotational spectroscopy perspective, cases involving two quadrupolar nuclei pose a significant challenge as the hyperfine patterns can be quite complex. A survey of the literature shows a number of examples in which the hyperfine structure of molecules with two chlorine atoms has been investigated via microwave spectroscopy in the last seven decades.[7–23] In the earliest studies, as Stark modulated microwave spectrometers measured line positions to only a few hundreds of kHz, the splitting patterns were only partially resolved for a few transitions or the spectral analysis was completed with only one hyperfine component for each transition.[18–20] More recently, the improved resolution of Fourier transform microwave (FTMW) spectrometers has enabled more comprehensive studies of dichlorinated species[9–12,21–23] and their weakly bound complexes.[13–15]

Our interest in 2,5-dichlorothiophene (DCT), as detailed in this paper, addresses the challenge of assigning complex hyperfine structure arising from two chlorine nuclei for a species that has, before now, never been studied via high resolution spectroscopy. Careful analysis of the splitting patterns yielded accurate χ values for diagonal and off-diagonal elements of the nuclear quadrupole coupling tensor for the ^{35}Cl-^{35}Cl, ^{37}Cl-^{35}Cl and ^{37}Cl-^{37}Cl isotopic species and the ^{34}S and two ^{13}C analogues of the ^{35}Cl-^{35}Cl containing compound. Using the experimental rotational constants of the isotopologues, the substitution (r_s), ground state effective (r_0) and mass-weighted ($r_m^{(1)}$) geometries of DCT were derived for comparison with the equilibrium structure (r_e) predicted using MP2/aug-cc-pVTZ calculations. Compared with thiophene, the S-C-C angles and S-C bond lengths are slightly larger in DCT which is rationalized using natural bond orbital (NBO) analysis to deduce the changes in the electronic structure that accompany chlorine substitution.

Experimental Methods

DCT was purchased from Sigma-Aldrich Canada (98%; bp 162˚C) and used to prepare a gas mixture by flowing the neon carrier gas through a glass bubbler at a pressure of ~1 bar. The seeded neon was introduced into the high vacuum chamber of the spectrometers as a supersonic jet expansion using a General Valve Series 9 pulsed nozzle. The pure rotational spectrum of DCT was then recorded using our chirped pulse (cp)[24] and Balle-Flygare (BF)[25] Fourier transform microwave (FTMW) spectrometers. The cp-FTMW instrument was initially used to measure a low resolution (~200 kHz FWHM), broadband spectrum from 7-19 GHz in segments of 2 GHz. This survey spectrum enabled preliminary assignment of clusters of rotational transitions corresponding to the three chlorine isotopic variations of DCT (^{35}Cl-35Cl, ^{37}Cl-^{35}Cl, and ^{37}Cl-^{37}Cl) and the ^{34}S and two ^{13}C analogues of the first of these. The higher resolution BF-FTMW spectrometer (~7 kHz FWHM) was then used to investigate the patterns of hyperfine transitions within each cluster of lines resulting in a more precise determination of frequencies to within ±3 kHz typically and to measure lower frequency transitions down to 5.5 GHz. Transitions measured using the BF instrument are split into a Doppler pair because of the coaxially oriented arrangement of the supersonic jet and resonator axis. The line position is obtained as the arithmetic mean of the frequencies of the Doppler components. All assigned transitions are given as Supporting Information.

Computational Methods

The equilibrium geometry of DCT and relevant spectroscopic constants, including the chlorine nuclear quadrupole hyperfine constants, were predicted using *ab initio* calculations at the MP2/aug-cc-pVTZ level of theory in Gaussian 16 Revision C.01[26] for each of the three isotopologues. This method was chosen following some preliminary benchmarking tests of similar-sized basis sets at the MP2 and B3LYP levels of theory to determine which could best predict the experimental rotational and ^{35}Cl nuclear quadrupole coupling constants of 2-chlorothiophene.[5] The geometry optimization calculations for the isotopologues of DCT were followed by harmonic frequency calculations to ensure that the structures corresponded to a minimum and to estimate the quartic centrifugal distortion constants. The key spectroscopic parameters are summarized in Tables 1 and 2 and the internal coordinates of the six isotopologues of DCT are given in the Supporting Information. Natural bond orbital (NBO)[27] analysis was also performed on the optimized structures of DCT, 2-chlorothiophene and thiophene at the B3LYP-D3(BJ)\aug-cc-pVTZ level to deduce the relationship between the electronic properties and geometry of DCT.

Results

DCT is a planar molecule with a substantial dipole along the *b*-inertial axis (0.997 D, MP2/aug-cc-pVTZ) upon which the sulfur atom sits. The two chlorine atoms are equivalent in the ^{35}Cl-^{35}Cl and ^{37}Cl-^{37}Cl isotopologues but not in the case of ^{37}Cl-^{35}Cl. Considering the natural occurrence of the ^{35}Cl and ^{37}Cl isotopes of 75.5% and 24.3%, respectively, the relative abundance of the ^{35}Cl-^{35}Cl, ^{37}Cl-^{35}Cl, and ^{37}Cl-^{37}Cl isotopologues is 9:6:1. This ratio takes into account that the ^{37}Cl in the ^{37}Cl-^{35}Cl isotopic species can be substituted on either side of sulfur in the ring. As seen in Figure 1 which displays a portion of the broadband spectrum collected with the cp-FTMW spectrometer, clusters of transitions were readily observed that matched this ratio. These clusters arise from the chlorine nuclear quadrupole hyperfine structure of a particular *b*-type rotational transition (in this case J' K_a' K_c'-J'' K_a'' K_c''=3_{13}-2_{02}). Transitions due to the ^{34}S and two ^{13}C isotopologues (with ^{35}Cl-^{35}Cl) were also recorded with intensities that were ~4% and ~2% of the

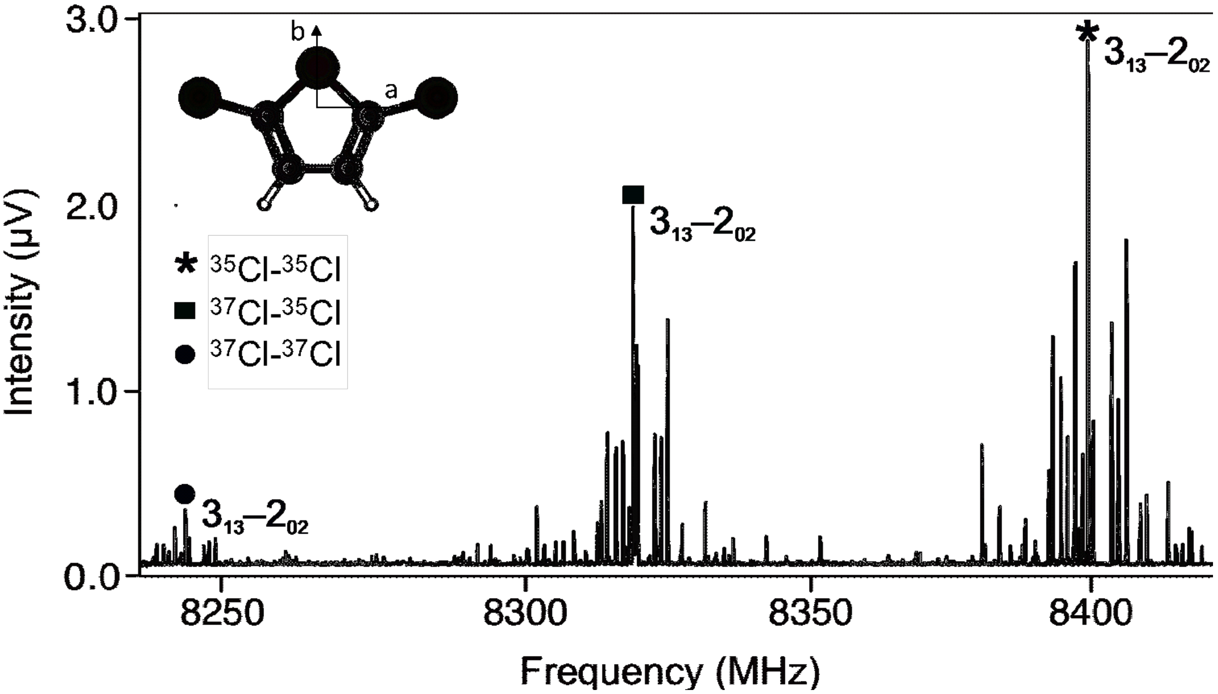

Figure 1. Portion of cp-FTMW spectrum (from averaging 1.5 million FIDs) depicting the chlorine nuclear quadrupole hyperfine patterns for the three isotopologues of DCT.

main isotopologue as expected based on the isotopic abundance and the symmetry of the DCT providing two equivalent C_α and C_β.

For the ^{35}Cl-^{35}Cl and ^{37}Cl-^{37}Cl species, which have equivalent quadrupolar nuclei (I_1=I_2), the total angular momentum (F) used for labelling the hyperfine transitions in the analysis combines the rotational angular momentum (J) with the total nuclear spin (I_t) as follows:

$$\overrightarrow{I_1} + \overrightarrow{I_2} = \overrightarrow{I_t}\,;\ \ \overrightarrow{I_t} + \vec{J} = \vec{F}$$

while the treatment in the case of the mixed ^{37}Cl-^{35}Cl isotopologue ($I_1 \neq I_2$) used the scheme:

$$\overrightarrow{I_1} + \vec{J} = \overrightarrow{F_1}\,;\ \ \overrightarrow{F_1} + \overrightarrow{I_2} = \vec{F}$$

Following these labelling conventions, the complex hyperfine patterns were simulated using *ab initio* estimates of the nuclear quadrupole coupling constants (χ) for the ^{35}Cl-^{35}Cl, ^{37}Cl-^{35}Cl, and ^{37}Cl-^{37}Cl species from Tables 1 and 2 and these were compared with the experimental spectrum. By first identifying the most intense hyperfine features of a few prominent rotational transitions, a full assignment was soon realized. Figure 2 demonstrates the excellent agreement between the simulated and experimental hyperfine patterns for the 3_{13}-2_{02} rotational transition of ^{35}Cl-^{35}Cl DCT.

The observed transitions for each isotopologue of DCT were fit using Pickett's SPFIT program[28] with Watson's A-reduced Hamiltonian[29] I^r representation and the resulting constants are compiled in Tables 1 and 2 while the observed frequencies are provided as Supporting Information. The equivalence of the two chlorine nuclei in the ^{35}Cl-^{35}Cl and ^{37}Cl-^{37}Cl isotopologues was considered by requiring the magnitude of their χ values to be the same during the fit while constraining the χ_{ab} off-diagonal terms to be of opposite sign. In the end, the rms errors of the six fits are less than 2 kHz which indicates that the employed model Hamiltonian does an excellent job of accounting for the complex splitting patterns of the isotopologues. Although the sulfur atom is shifted slightly (0.035 Å, MP2/aug-cc-pVTZ) off the *b*-axis in the ^{37}Cl-^{35}Cl isotopologue due to the different center of mass, this subtle symmetry-breaking change did not permit observation of *a*-type transitions as $|\mu_a|$ was estimated to be negligible (0.002 D, MP2/aug-cc-pVTZ).

Furthermore, as each rotational transition is split into a large number of hyperfine components, we could not identify features due to the remaining minor isotopic species including those with ^{34}S and ^{13}C substitution.

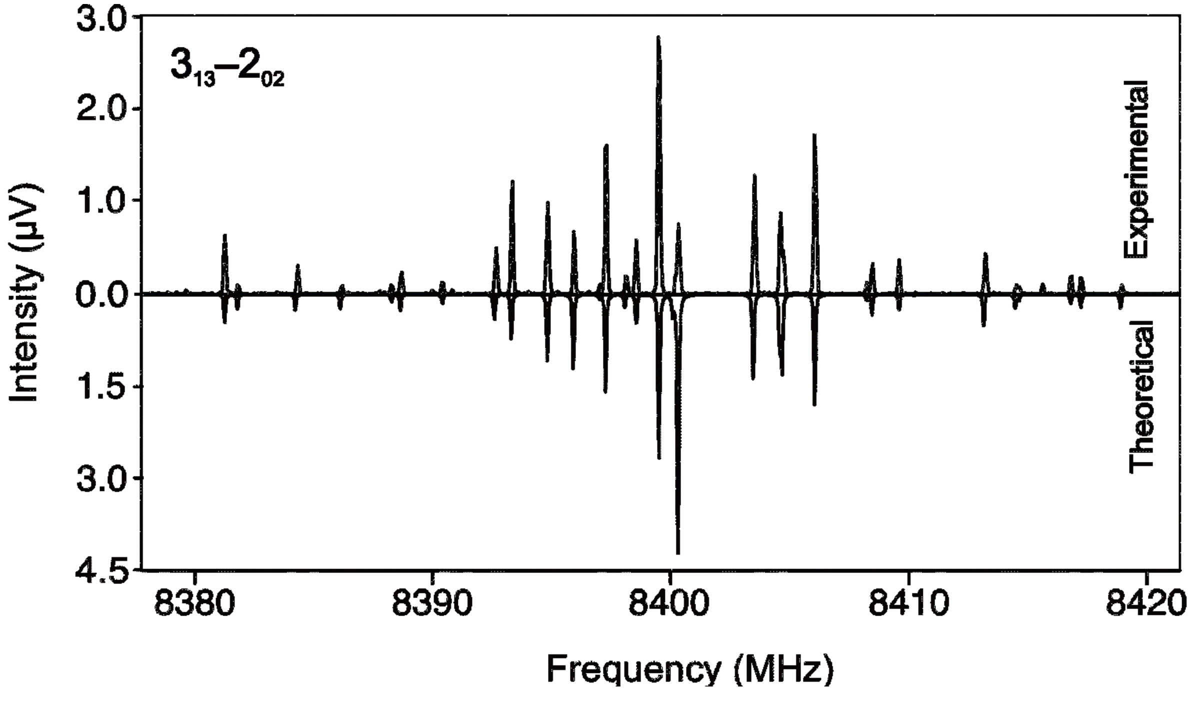

Figure 2. Comparison of the predicted and experimental nuclear quadrupole hyperfine structure of a single rotational transition of ^{35}Cl-^{35}Cl DCT.

Table 1. Experimental (A-Reduced I^r Representation) and Theoretical (MP2/aug-cc-pVTZ) Spectroscopic constants of the Cl Isotopologues of DCT with 1σ Uncertainties in Parentheses.

	ab initio			experiment		
	^{35}Cl-^{35}Cl	^{37}Cl-^{35}Cl	^{37}Cl-^{37}Cl	^{35}Cl-^{35}Cl	^{37}Cl-^{35}Cl	^{37}Cl-^{37}Cl
A /MHz	5002	4997	4992	4998.956162(38)	4994.561332(42)	4990.020188(71)
B	800.9	780.5	760.8	802.180493(28)	781.958088(31)	762.243911(63)
C	690.4	675.4	660.2	691.185920(26)	676.039390(29)	661.173941(48)
Δ_J /kHz	0.01668	0.01595	0.01525	0.01722(21)	0.01650(26)	0.01689(55)
Δ_K	1.562	1.587	1.606	[1.562][a]	[1.587] [a]	[1.606][a]
Δ_{JK}	−0.002222	−0.005720	−0.009196	[−0.002222][a]	[−0.005720][a]	[−0.009196][a]
δ_J	0.002911	0.002733	0.002566	[0.002911][a]	[0.002733] [b]	[0.002566] [a]
δ_K	0.09323	0.08964	0.08615	[0.09323][a]	[0.08964][a]	[0.08615][a]
Cl(1) 3/2 χ_{aa} /MHz	−97.466	−76.965 (^{37}Cl)	−76.832	−103.5166(13)	−81.7294(40) (^{37}Cl)	−81.5838(35)
Cl(2) 3/2 χ_{aa}	−97.466	−97.317 (^{35}Cl)	−76.832	{−103.5166(13)}[b]	−103.3328(35) (^{35}Cl)	{−81.5838(35)}[b]
Cl(1)1/4(χ_{bb}−χ_{cc})	−1.464	−1.134 (^{37}Cl)	−1.156	−1.40085(24)	−1.08070(53) (^{37}Cl)	−1.10436(51)
Cl(2) 1/4(χ_{bb}−χ_{cc})	−1.464	−1.496 (^{35}Cl)	−1.156	{−1.40085(24)}[b]	−1.43091(47) (^{35}Cl)	{−1.10436(51)} [b]
Cl(1) χ_{ab}	25.267	−19.763 (^{37}Cl)	−19.930	27.3051(32)	−21.329(18) (^{37}Cl)	−21.525(19)
Cl(2) χ_{ab}	-25.267	25.499 (^{35}Cl)	19.930	{−27.3051(32)}[c]	27.536(15) (^{35}Cl)	{21.525(19)}[c]
No. of lines	−	−	−	345	320	109
rms /kHz	−	−	−	1.5	1.5	1.5

[a]Parameter fixed at the *ab initio* value; [b]Set as equal to value for other Cl nucleus during fit; [c]Set as equal in magnitude but opposite sign to the value of the other Cl.[30]

Table 2. Experimental (A-Reduced I^r Representation) and Theoretical (MP2/aug-cc-pVTZ) Spectroscopic Constants of the ^{34}S and ^{13}C Isotopologues of DCT (with ^{35}Cl-^{35}Cl) with 1σ Uncertainties in Parentheses.

	ab initio			experiment		
	^{34}S	^{13}C$_\alpha$	^{13}C$_\beta$	^{34}S	^{13}C$_\alpha$	^{13}C$_\beta$
A /MHz	4910	4999	4893	4906.74710(16)	4996.44989(41)	4890.60341(39)
B	800.9	799.0	800.3	802.19413(14)	800.31726(35)	801.53576(33)
C	688.6	688.9	687.8	689.404267(50)	689.75517(10)	688.596924(94)
Δ_J /kHz	0.01666	0.01659	0.01654	[0.01666] [a]	[0.01659] [a]	[0.01654] [a]
Δ_K	1.421	1.577	1.528	[1.421] [a]	[1.577] [a]	[1.528] [a]
Δ_{JK}	0.007805	−0.003410	−0.002526	[0.007805] [a]	[−0.003410] [a]	[−0.002526] [a]
δ_J	0.002918	0.002894	0.002947	[0.002918] [a]	[0.002894] [a]	[0.002947] [a]
δ_K	0.09341	0.09254	0.09182	[0.09341] [a]	[0.09254] [a]	[0.09182] [a]
$3/2\ \chi_{aa}$ /MHz	−97.466	−97.506	−97.618	−103.5035(67)	−103.516(16)	−103.541(13)
$1/4(\chi_{bb}-\chi_{cc})$	−1.464	−1.458	−1.439	−1.4014(11)	−1.4006(20)	−1.4049(21)
χ_{ab}	±25.267	±25.217	±25.077	±27.328(29)	±27.306(28)	±27.34(10)
No. of lines				52	30	28
rms /kHz				1.9	2.0	1.8

[a] Parameter fixed at the *ab initio* value.

With accurate sets of experimental rotational constants for six isotopologues in Tables 1 and 2, the geometry of DCT was estimated via Kraitchmann's equations (r_s)[31] and direct least squares fitting of the moments of inertia to structural parameters (r_0, $r_m^{(1)}$)[32,33] as described below. Due to the C_{2v} symmetry of DCT, very few parameters are actually needed to describe the geometry of the ring and as the molecule is planar, only two rotational constants from each set are linearly independent. First, the absolute values of the Kraitchman coordinates for each heavy atom (along with their respective Costain errors)[34] were determined with Kisiel's KRA program[35,36] by using the average coordinates obtained from consideration of each of the three pairs of rotational constants (AB, AC, BC) as advocated in the study of 1,2-dichlorobenzene.[12] As S lies on the b-axis of DCT, its a-coordinate was imaginary and set to zero. The signs of the coordinates were then inferred using the *ab initio* equilibrium geometry (r_e) of DCT and the resulting atomic positions were used to calculate the internal coordinates of DCT and their 1σ uncertainties using the EVAL routine.[35,36] These are listed under the r_s heading in Table 3. Next, the effective ground state (r_0) structure was estimated by least squares fitting of the moments of inertia using Kisiel's STRFIT program[35,36] again by averaging the results from three data sets (AB, AC, BC) and by requiring maintenance of C_{2v} symmetry. In this procedure, the bond lengths and angles involving hydrogen were fixed to their *ab initio* values and any parameters that were not directly fit were subsequently calculated from the final set of atomic positons; the results summarized in Table 3. Finally, the mass-weighted geometry ($r_m^{(1)}$) was derived from the full set of 18 rotational constants in an effort to provide a more meaningful account of the vibrational effects. In comparing the r_0 and $r_m^{(1)}$ geometries in Table 3, the standard deviation of individual internal coordinates is reduced by the inclusion of empirical parameters (c_a, c_b, c_c)[33] in the latter as expected but some of these bond lengths and angles change by significantly more than their nominal precision as noted also in the study of 1,2-dichlorobenzene.[12]

Table 3. Comparison of the Experimental (r_s, r_0, $r_m^{(1)}$) and Theoretical (r_e) (MP2/aug-cc-pVTZ) Geometry of DCT, 2-Chlorothiophene (2CT) and Thiophene (T) with Bond Distances in Å and Bond Angles in Degrees with 1σ Uncertainties in Parentheses.

	r_S DCT	r_0 DCT	$r_m^{(1)}$ DCT	r_e DCT	r_e 2CT	r_e thiophene
R(C_2-S)	1.712(5)	1.719(8)	1.715(4)	1.723	1.717	1.711
R(C_2-Cl)	1.720(3)	1.711(3)	1.719(2)	1.712	1.714	
R(C_2-C_3)	1.369(6)	1.376(6)	1.362(3)	1.375	1.377	1.378
R(C_3-C_4)	1.424(3)	1.429(14)	1.429(3)	1.415	1.413	1.413
<S-C_2-Cl	120.2(4)	120.4(6)	120.0(2)	120.2	120.6	
<S-C_2-C_3	113.4(1)	113.0(6)	113.5(1)	112.5	112.4	111.4
<C_2-S-C_5	90.2(2)	90.7(3)	90.1(1)	90.7	91.4	92.3
<C_2-C_3-C_4	111.5(2)	111.7(6)	111.5(1)	112.1	111.5	112.5
N_{par}[a]		5	8			
σ_{fit}[b]		0.012	0.0039			

[a]Number of independent parameters in the fit; [b]Standard deviation of fit

Discussion

In this work, the ground state rotational, centrifugal distortion and nuclear quadrupole coupling constants of the six isotopologues of DCT were precisely determined for the first time via microwave spectroscopy. The experimentally-derived rotational constants in are within 0.2% of the equilibrium rotational constants (MP2/aug-cc-pVTZ) suggesting that the experimental geometry is similar to the equilibrium (r_e) structure of DCT. The inertial defects (Δ_0=0.073 uÅ^2) and planar moments (P_{cc}=−0.037 uÅ^2) are the same for all three isotopic species and point to a planar molecule as expected.

The parameters related to the chlorine nuclear quadrupole coupling constants in Tables 1 and 2 have been separated into the individual tensor components in Table 4 in the principal inertial frame (a, b, c) and transformed also into the chlorine field gradient frame (x, y, z) through diagonalization of the matrix using QDIAG.[35,36] Comparison of these values with the *ab initio* estimates (also in Table 4) show that while the correct trends are captured by quantum chemical calculations, the experimental χ values differ from the theoretical estimates by as much as 8%. Similar large discrepancies are noted in nuclear quadrupole parameters of chlorine in the literature when common computational methods are employed as seen in chloroform[37] for example where the experimentally derived χ_{zz} value differed by 13% from the prediction (MP2/aug-cc-pVDZ). This was attributed to the failure of Gaussian-type orbital basis functions at capturing the sharp cusp in electron density at the quadrupolar nucleus.[22] When employing standard computational methods, ad hoc scaling factors have been shown to compensate for this shortcoming but these factors are dependent on the theory and basis set employed as shown in a comprehensive study of chlorine-containing species.[37] As two-thirds of the NMR-active nuclei in the periodic table are quadrupolar in nature,[3] this challenge in modelling key parameters for seemingly simple molecules with widely accessible computational tools is noteworthy. Future efforts to improve the reliability of 'blackbox' calculations for nuclei like chlorine based on results from gas phase measurements would, no doubt, be of great interest to both the NMR and molecular spectroscopy communities.

The chlorine nuclear quadrupole coupling constants of DCT provide important structural details for this planar molecule. The component of the tensor perpendicular to the plane of the ring should be constant for a specific isotope and this is confirmed by the χ_{cc} values in Table 4. The ^{35}Cl/^{37}Cl ratio of χ_{cc} is 1.268 which is in good agreement with the value reported for 2CT[5] and other chlorine-containing species.[38] The angle θ_{za} between the inertial *a*-axis of DCT and the z-axis of the chlorine quadrupole coupling tensor for the parent species in Table 4, −14.2338(14)°, is very similar to the angle θ_{str} between the C-Cl bond and the a-axis of the molecule, -15.0(7)°, derived from the r_0 geometry (and in agreement with the ab initio estimates) which indicates that the z-axis of the chlorine field gradient is nearly aligned with the C-Cl bond. This is further confirmed by the small nuclear quadrupole asymmetry parameter $\eta = (\chi_{xx} - \chi_{yy})/\chi_{zz}$ in DCT (−0.017457(32)) which indicates that the electric field gradient at chlorine is nearly cylindrically symmetric about the C-Cl bond.

Table 4. Chlorine Nuclear Quadrupole Coupling Constants and Related Parameters for the Isotopologues of DCT with 1σ uncertainties in parentheses.

	^{35}Cl-^{35}Cl	^{35}Cl-^{35}Cl	^{35}Cl-^{37}Cl		^{37}Cl-^{37}Cl	^{34}S(^{35}Cl-^{35}Cl)	^{13}C$_{\alpha}$(^{35}Cl-^{35}Cl)	^{13}C$_{\beta}$(^{35}Cl-^{35}Cl)
	ab initio[a]		^{35}Cl	^{37}Cl				
χ_{aa} /MHz	−64.977	−69.0111(13)	-68.8885(35)	−54.4863(40)	−54.3892(35)	−69.0023(67)	−69.011(16)	−69.027(13)
χ_{bb}	29.561	31.7039(13)	31.5824(35)	25.0818(40)	24.9859(35)	31.6983(68)	31.704(16)	31.704(13)
χ_{cc}	35.417	37.3072(13)	37.3061(35)	29.4045(40)	29.4033(35)	37.3040(68)	37.307(16)	37.323(13)
χ_{ab}	±25.267	±27.3051(32)	27.536(15)	−21.329(18)	±21.525(19)	±27.328(29)	±27.306(28)	±27.34(10)
χ_{zz}	−71.306	−75.9375(20)	−75.9403(79)	−59.8431(93)	−59.8506(96)	−75.941(15)	−75.938(20)	−75.969(49)
χ_{xx}	35.890	38.6303(20)	38.6342(79)	30.4386(93)	30.4473(96)	38.637(15)	38.631(20)	38.646(49)
χ_{yy}	35.417	37.3072(13)	37.3061(35)	29.4045(40)	29.4033(34)	37.3040(68)	37.307(16)	37.323(13)
θ_{za} /°	14.063	14.2338(14)	14.3644(66)°	14.098(10)°	14.237(11)°	14.246(13)°	14.234(13)°	14.247(44)°
θ_{str}	15.088	15.0(7)						
η	−0.006637	−0.017457(32)	−0.01749(11)	−0.01728(17)	−0.01744(17)	−0.01755(22)	−0.01743(34)	−0.01742(67)

[a] MP2/aug-cc-pVTZ

Comparison of the three experimental geometries with the equilibrium structure (r_e) for DCT in Table 3, reveals that the r_0 method provides a good estimate of the arrangement of heavy atoms with all internal coordinates agreeing to within 1σ of the theoretical values. The geometry of DCT is remarkably similar to those of the related compounds thiophene and 2-chlorothiophene (2CT); the relevant r_e parameters for the latter two were calculated in this work and are also included in Table 3 for comparison. The most significant change in the ring backbone is seen for the $<C_2$-S-C_5 angle which decreases by 1.6° from thiophene to DCT. This is seemingly driven by changes in the electronic structure at the neighboring sites where the chlorine substitution occurs as both the <S-C_2-C_3 angle and R(C_2-S) bond length (and the equivalent parameters by symmetry) increase by 1.1° and 0.012 Å, respectively. Similar structural effects are noted at C_2 in 2CT in comparison to the parent compound. The increase in the ring angle at the site of chlorination is smaller than has been reported for fluorination on aromatic rings (2-3°).[39–47] This was previously explained in terms of the polarity of the C-X bond as a result of the inclusion on an electron withdrawing substituent (X). This change results in more p-character in the hybrid orbital centered on the carbon directed towards the halogen atom. In DCT and 2CT, for example, the character of this orbital directed at chlorine is $sp^{2.6}$ based on NBO analysis compared with sp^2 hybridization in thiophene. More unexpected is the slight lengthening of the C_2-S bond in the chlorinated compounds as the ring opening at the halogenation site is normally accompanied by shortening of the adjacent bonds due to the increased s-character in the hybrid orbitals on C_2 directed to neighboring atoms within the ring itself. In this case, the shorter C-S bond in the thiophene parent is consistent with the larger difference in natural charges on C_2 (−0.415) and S (0.450) compared with those in DCT (C_2: −0.273, S: 0.491) and 2CT (C_2: −0.278, S: 0.473) resulting from the electron withdrawing properties of chlorine.

Conclusion

The rotational spectrum of DCT, including transitions of the ^{35}Cl-^{35}Cl, ^{37}Cl-^{35}Cl and ^{37}Cl-^{37}Cl isotopologues, was recorded and its complex patterns of transitions arising from two quadrupolar chlorine nuclei were analysed to derive accurate experimental nuclear quadrupolar coupling constants. The results show that the experimentally-derived χ values differ from theoretical predictions (MP2/aug-cc-pVTZ level of theory) by as much as 8% suggesting that further studies that provide benchmark data of this type are worthwhile to improve the accuracy of modelling NMR properties of quadrupolar nuclei. The experimental geometry of DCT, in comparison to thiophene, reveals small changes to the ring when the electron withdrawing chlorine atoms are added in the *ortho* positions including a 1.1° increase in the <S-C-C angles and a 0.012 Å increase in the S-C bond lengths. The subtle changes in the ring angles at the sites of chlorination in DCT may be constrained by the geometry of the five-membered ring to some extent as halogen substitution on six-membered rings has shown changes that are two to three times larger.[39–41]

Supporting Information

Cartesian coordinates for DCT (MP2/aug-cc-pVTZ)

Observed frequencies and residuals of the fit of DCT

Tabulated output of r_0 geometry determination

Tabulated output of $r_m^{(1)}$ geometry determination

Acknowledgements

This research was funded by the Natural Sciences and Engineering Research Council of Canada (NSERC) through the Discovery Grants program (JvW) and through a summer Undergraduate Research Award (GD) through the VP Research Office at the University of Manitoba. We are grateful for computational support from W. G. D. P. Silva.

References

(1) *The Organic Chemistry of Drug Synthesis*; Lednicer, D., Mitscher, L. A., Eds.; Wiley Interscience: New York, 1977.

(2) Chen, W.; Caceres-Cortes, J.; Zhang, H.; Zhang, D.; Humphreys, W. G.; Gan, J. Bioactivation of Substituted Thiophenes Including α-Chlorothiophene- Containing Compounds in Human Liver Microsomes. *Chem. Res. Toxicol.* **2011**, *24* (5), 663–669.

(3) Bryce, D. L.; Sward, G. D. Solid-State NMR Spectroscopy of the Quadrupolar Halogens: Chlorine-35/37, Bromine-79/81, and Iodine-127. *Magn. Reson. Chem.* **2006**, *44* (4), 409–450.

(4) Bryce, D. L.; Wasylishen, R. E. Microwave Spectroscopy and Nuclear Magnetic Resonance Spectroscopy- What Is the Connection? *Accounts Chem. Res.* **2003**, *36* (5), 327–334.

(5) Mjöberg, J.; Ljunggren, S. Microwave Spectrum and Quadrupole Coupling Constants of 2-Chlorothiophene. *Zeitschrift fur Naturforsch. - Sect. A J. Phys. Sci.* **1973**, *28a*, 729–738.

(6) Niide, Y.; Ohkoshi, I. Microwave Spectrum and Quadrupole Coupling Constant Tensor of 3-Chlorothiophene. *J. Mol. Spectrosc.* **1988**, *130*, 46–53.

(7) Wilse Robinson, G. The Microwave Spectrum of Phosgene. *J. Chem. Phys.* **1953**, *21* (10), 1741–1745.

(8) Takeo, H.; Matsumura, C. The Microwave Spectrum of Dichlorodifluoromethane. *Bull. Chem. Soc. Jpn.* **1977**, *50* (3), 636-640.

(9) Van Wynsberghe, A. W.; Peebles, S. A.; Peebles, R. A.; Kuczkowski, R. L. Rotational Spectrum and Structure of 1,2-Dichloro-3,3,4,4-Tetrafluorocyclobutene: Comparison of Spectroscopy, Diffraction, and Ab Initio Results. *J. Phys. Chem. A* **2000**, *104* (38), 8702–8708.

(10) Hansen, N.; Mäder, H.; Temps, F. The Rotational Spectrum of Dichlorocarbene, $C^{35}Cl_2$, Observed by Molecular Beam-Fourier Transform Microwave Spectroscopy. *Phys. Chem.*

Chem. Phys. **2001**, *3* (1), 50–55.

(11) Białkowska-Jaworska, E.; Pszczółkowski, L.; Kisiel, Z. Comprehensive Analysis of the Rotational Spectroum of 2 ,2-Dichloropropane. *J. Mol. Spectrosc.* **2015**, *308–309*, 20–207.

(12) Kisiel, Z.; Białkowska-Jaworska, E.; Chen, J.; Pszczółkowski, L.; Gawryś, P.; Kosarzewski, J. Rotational Spectroscopy and Precise Molecular Structure of 1,2-Dichlorobenzene. *J. Mol. Spectrosc.* **2020**, *374*, 111380.

(13) Velino, B.; Evangelisti, L.; Caminati, W.; Fausto, R. Conformation, Structure, Quadrupole Coupling Constants and van Der Waals Potential Energy Surface of Dichloromethane-Ar. *J. Mol. Struct.* **2010**, *976* (1–3), 136–140.

(14) Kisiel, Z.; Lesarri, A.; Neill, J. L.; Muckle, M. T.; Pate, B. H. Structure and Properties of the $(HCl)_2H_2O$ Cluster Observed by Chirped-Pulse Fourier Transform Microwave Spectroscopy. *Phys. Chem. Chem. Phys.* **2011**, *13* (31), 13912–13919.

(15) Favero, L. B.; Maris, A.; Paltrinieri, L.; Caminati, W. Rotational Spectrum of Dichloromethane-Ne: Internal Dynamics and Cl Quadrupolar Hyperfine Effects. *J. Phys. Chem. A* **2015**, *119* (49), 11813–11819.

(16) Caminati, W.; Fantoni, A. C.; Lunelli, B.; Scappini, F. Radiofrequency-Microwave Double Resonance with a Dipole Moment Component Induced by Asymmetric Isotopic Substitution: Microwave Spectrum of $C_4O_2Cl_2$. *J. Mol. Spectrosc.* **1988**, *131* (1), 154–160.

(17) Tanimoto, M.; Takeo, H.; Matsumura, C.; Fujitake, M.; Hirota, E. Microwave Spectroscopic Detection of Dichlorosilylene $SiCl_2$ in the Ground State. *J. Chem. Phys.* **1989**, *91* (4), 2102–2107.

(18) Myers, R. J.; Gwinn, W. D. The Microwave Spectra, Structure, Dipole Moment, and Chlorine Nuclear Quadrupole Coupling Constants of Methylene Chloride. *J. Chem. Phys.* **1952**, *20* (9), 1420–1427.

(19) Flygare, W. H.; Narath, A.; Gwinn, W. D. Microwave Spectrum, Structure, Quadrupole

Interaction, Dipole Moment, and Bent C-Cl Bonds in 1,1-Dichlorocyclopropane. *J. Chem. Phys.* **1962**, *36* (1), 200–208.

(20) Takeo, H.; Sugie, M.; Matsumura, C. Microwave Spectra and Structure of Dichloroethenes. *J. Mol. Struct.* **1988**, *190*, 205–214.

(21) Kisiel, Z.; Kosarzewski, J.; Pszczólkowski, L. Nuclear Quadrupole Coupling Tensor of CH_2Cl_2: Comparison of Quadrupolar and Structural Angles in Methylene Halides. *Acta Phys. Pol. A* **1997**, *92* (3), 507–516.

(22) Kisiel, Z.; Białkowska-Jaworska, E.; Pszczółkowski, L. Nuclear Quadrupole Coupling in Cl_2CCHCl and Cl_2CCH_2: Evidence for Systematic Differences in Orientations between Internuclear and Field Gradient Axes for Terminal Quadrupolar Nuclei. *J. Chem. Phys.* **1998**, *109* (23), 10263–10272.

(23) De Luis, A.; López, J. C.; Alonso, J. L. The Cl-Nuclear Quadrupole Coupling Tensors and the Internal Rotation Barrier of 1,1-Dichloroethane by Fourier Transform Microwave Spectroscopy. *Chem. Phys.* **1999**, *248* (2–3), 247–261.

(24) Evangelisti, L.; Sedo, G.; van Wijngaarden, J. Rotational Spectrum of 1,1,1-Trifluoro-2-Butanone Using Chirped-Pulse Fourier Transform Microwave Spectroscopy. *J. Phys. Chem. A* **2011**, *115* (5), 685–690.

(25) Sedo, G.; van Wijngaarden, J. Fourier Transform Microwave Spectra of a “New” Isomer of $OCS-CO_2$. *J. Chem. Phys.* **2009**, *131* (4), 044303.

(26) Frisch, M. J.; Trucks, G. W.; Schlegel, H. B.; Scuseria, G. E.; Robb, M. A.; Cheeseman, J. R.; Scalmani, G.; Barone, V.; Petersson, G. A.; Nakatsuji, H.; et al. Gaussian 16 Revision C.01. Gaussian Inc.: Wallingford CT 2016.

(27) Glendening, E. D.; Badenhoop, J. K.; Reed, A. E.; Carpenter, J. E.; Bohmann, J. A.; Morales, C. M.; Karafiloglou, P.; Landis, C. R.; Weinhold, F. NBO 7.0. Theoretical Chemistry Institute, University of Wisconsin: Madison, WI 2018.

(28) Pickett, H. M. The Fitting and Prediction of Vibration-Rotation Spectra with Spin

Interactions. *J. Mol. Spectrosc.* **1991**, *148* (2), 371–377.

(29) Watson, J. K. G. Determination of Centrifugal Distortion Coefficients of Asymmetric-Top Molecules. III. Sextic Coefficients. *J. Chem. Phys.* **1968**, *48* (10), 4517–4524.

(30) Spoerel, U.; Dreizler, H.; Stahl, W. On the Sign of the Off-Diagonal Elements of the Nuclear Quadrupole Coupling Tensor. *Z. Naturforsch.* **1994**, *49a*, 645–646.

(31) Kraitchman, J. Determination of Molecular Structure from Microwave Spectroscopic Data. *Am. J. Phys.* **1953**, *21* (1), 17–24.

(32) Schwendeman, R. H. Structural Parameters from Rotational Spectra. In *Critical Evaluation of Chemical and Physical Structural Information*; Lide, D. R.; Paul, M. A., Ed.; National Academies Press, 1974; pp 94–115.

(33) Watson, J. K. G.; Roytburg, A.; Ulrich, W. Least-Squares Mass-Dependence Molecular Structures. *J. Mol. Spectrosc.* **1999**, *196* (1), 102–119.

(34) Costain, C. C. Further Comments on the Accuracy of r_s Substitution Structures. *Trans. Am. Crystallogr. Assoc.* **1966**, *2*, 157–164.

(35) Kisiel, Z. Assignment and Analysis of Complex Rotational Spectra. In *Spectroscopy from Space*; Demaison, J., Sarka, K., Cohen, E. A., Eds.; Springer, 2001; pp 91–106.

(36) Kisiel, Z. PROSPE - Programs for ROtational SPEctroscopy http://www.ifpan.edu.pl/~kisiel/prospe.htm (accessed Aug 3, 2020).

(37) Białkowska-Jaworska, E.; Kisiel, Z.; Pszczółkowski, L. Nuclear Quadrupole Coupling in Chloroform and Calibration of Ab Initio Calculations. *J. Mol. Spectrosc.* **2006**, *238* (1), 72–78.

(38) Gordy, W.; Cooke, R. L. *Microwave Molecular Spectra*, 3rd ed.; Wiley: New York, 1984.

(39) van Dijk, C. W.; Sun, M.; van Wijngaarden, J. Microwave Rotational Spectra and Structures of 2-Fluoropyridine and 3-Fluoropyridine. *J. Phys. Chem. A* **2012**, *116* (16), 4082–4088.

(40) van Dijk, C. W.; Sun, M.; van Wijngaarden, J. Investigation of Structural Trends in

Difluoropyridine Rings Using Chirped-Pulse Fourier Transform Microwave Spectroscopy and Ab Initio Calculations. *J. Mol. Spectrosc.* **2012**, *280* (1), 34–41.

(41) Nygaard, L.; Bojesen, I.; Pedersen, T.; Rastrup-Andersen, J. Structure of Fluorobenzene. *J. Mol. Struct.* **1968**, *2* (3), 209–215.

(42) Poonia, T.; Silva, W. G. D. P.; van Wijngaarden, J. Derivation of an Accurate Geometry of 2-Fluoroaniline from Rotational Spectroscopy and Computational Chemistry. *J. Mol. Struct.* **2021**, *1225*.

(43) Bergmann, K.; van Wijngaarden, J. Rotational Spectroscopic and Ab Initio Investigation of the Rotamer Geometries of 2-Fluoroanisole and 3-Fluoroanisole. *ACS Appl. Mater. Interfaces* **2020**, No. 1.

(44) Kamaee, M.; Sun, M.; Luong, H.; van Wijngaarden, J. Investigation of Structural Trends in Mono-, Di-, and Pentafluorobenzonitriles Using Fourier Transform Microwave Spectroscopy. *J. Phys. Chem. A* **2015**, *119* (41), 10279–10292.

(45) Bell, A.; Singer, J.; Desmond, D.; Mahassneh, O.; van Wijngaarden, J. Rotational Spectra and Conformer Geometries of 2-Fluorophenol and 3-Fluorophenol. *J. Mol. Spectrosc.* **2017**, *331*, 53–59.

(46) Sun, W.; Lozada, I. B.; van Wijngaarden, J. Fourier Transform Microwave Spectroscopic and Ab Initio Study of the Rotamers of 2-Fluorobenzaldehyde and 3-Fluorobenzaldehyde. *J. Phys. Chem. A* **2018**, *122* (8), 2060–2068.

(47) Sun, W.; van Wijngaarden, J. Structural Elucidation of 2-Fluorothiophenol from Fourier Transform Microwave Spectra and Ab Initio Calculations. *J. Mol. Struct.* **2017**, *1144*, 496–501.